Analysis of natural vibration frequency of different support slabs under the traffic vibration based on field measurement

Qian Xia[1], Wenjun Qu[2,*], Yiqing Li[3], Jin Zhao[1]

1. School of Civil Engineering and Architecture, Xi'an University of Technology, Xi'an 710048, China

2. Department of structural Engineering, Tongji University, Shanghai 200092, China

3. Xi'an Jianda Weigu Quality Testing Technology Co. Ltd, Xi'an 710055, China

quwenjun.tj@tongji.edu.cn

ABSTRACT. *With the aid of the energy method, this paper calculates the natural vibration frequencies of precast and cast-in-situ plates in a residential building near a metro line in Shanghai, China, and sets up a detailed numerical model to verify the calculated results. The verification shows that the theoretical results on the natural vibration frequencies of floor slabs in different support modes agree well with the simulated results, an evidence to the correctness of the theoretical formulas based on the energy method. Based on the analysis results on the natural vibration frequencies floor slabs in different support modes, the author judged whether the slab vibrations, which make people uncomfortable, are caused by urban traffic excitation. The calculation and verification of the natural vibration frequencies floor slabs in different support modes provide valuable bases for vibration control and isolation of floor slabs in existing structures.*

RÉSUMÉ. *À l'aide de la méthode énergétique, cet article calcule les fréquences de vibration naturelle des plaques préfabriquées et coulées sur site dans un bâtiment résidentiel situé près d'une ligne de métro à Shanghai, en Chine, et établit un modèle numérique détaillé pour vérifier les résultats calculés. La vérification montre que les résultats théoriques sur les fréquences de vibration naturelles des planchers dans différents modes de support concordent bien avec les résultats simulés, ce qui prouve l'exactitude des formules théoriques basées sur la méthode de l'énergie. Sur la base des résultats d'analyse des fréquences de vibration naturelles des planchers dans différents modes de support, l'auteur a déterminé si les vibrations de la plancher, qui gênent les personnes, sont causées par l'excitation du trafic urbain. Le calcul et la vérification des fréquences de vibration naturelles des planchers dans différents modes de support fournissent des bases précieuses pour le contrôle des vibrations et l'isolation des planchers de sol dans les structures existantes.*

KEYWORDS: *energy method, natural vibration frequency, numerical simulation, theoretical calculation.*

MOTS-CLÉS: méthode de l'énergie, fréquence de vibration naturelle, simulation numérique, calcul théorique.

DOI:10.3166/I2M.17.219-233 © 2018 Lavoisier

1. Introduction

The vibration of floor slab is a heatedly discussed issue. Since Tredgold made the famous remark "girders should always be made as deep as they can to avoid the inconvenience of not being able to move on the floor without shaking everything in the room", much research has been done on the vibration of floor slab, especially that caused by urban transport (Hassan, 2008). However, it is still difficult to differentiate between the impact of urban transport factors from that of other factors (e.g. equipment vibration, rhythmic motion and nearby construction).

To overcome the difficulty, this paper adopts an innovative principle: the vibration of floor slab must be excited by a vibration source, as long as the natural vibration frequency of the floor slab falls in the frequency range of the floor slab vibration induced by that vibration source. Therefore, the natural vibration frequency of floor slab was computed accurately, aiming to determine whether a floor slab vibration, that makes people uncomfortable, originates from urban traffic. Here, the term natural frequency refers to the primary natural frequency of the vertical vibration of floor slab in a floor system with simple boundary conditions, while the term urban traffic is a collective term for all underground and surface vehicles in the urban road system.

2. Theoretical calculation

2.1. Basic assumptions and vibration differential equation

The floor slab is considered as a thin, isotropic and elastic plate that vibrates based on the following three assumptions:

(1) The straight line assumption: The lateral shear deformation is negligible, for all the points on the mid-plane normal of the plate are still on that normal after the bending deformation.

(2) The plate deflection is so much smaller than the plank thickness that the mid-plane will not deform when the plate is bent, i.e. the mid-plane is a neutral surface.

(3) The lateral positive stress of the plate is negligible compared with the positive stresses in the other two directions.

Under these assumptions, the plate deflection was calculated from the equilibrium position rather than the plane position, and the parallel hexahedrons in the plate were subjected to differential analysis. In this way, the bending equilibrium equation of the plate can be derived from the equilibrium conditions, deformation coordination conditions and other physical equations. After that, the differential equation of the plate's free vibration can be obtained through the analysis on the overall dynamic

equilibrium of the vibrating plate:

$$\frac{\partial^4 W}{\partial x^4}+2\frac{\partial^4 W}{\partial x^2\partial y^2}+\frac{\partial^4 W}{\partial y^4}+\frac{\overline{m}}{D}\frac{\partial^2 W}{\partial t^2}=0 \tag{1}$$

where W is the deflection function of the plate; $\overline{m}=\rho h$, with ρ being plate density and h being plate thickness; $D=Eh^3/12(1-v^2)$ is the flexural rigidity of the plate; E and v are the elastic modulus and Poisson's ratio of the plate, respectively; t is time variable. Each solution to equation (1) is the deflection of a point on the thin plate.

Let $W=\sum_{m=1}^{\infty}(A_m\cos\omega_m t+B_m\sin\omega_m t)F_m(x,y)$ be the superposed deflection under numerous vibration modes, with $F_m(x,y)$ being the shape function of the deflection under each mode. To obtain the shape function F_m under each mode and the corresponding circular frequency ω_m, the solution to equation (1) was assumed to be $W=F(x,y)(A\cos\omega t+B\sin\omega t)$. Substituting the solution into equation (1), we have:

$$\frac{\partial^4 F}{\partial x^4}+2\frac{\partial^4 F}{\partial x^2\partial y^2}+\frac{\partial^4 F}{\partial y^4}-\alpha^4 F=0 \tag{2}$$

where $\alpha^4=\omega^2\rho h/D$. Taking x=0 for instance, the corresponding boundary conditions are as follows:

Fixed edge: The displacement and rotation angle along the edge are zero, i.e. $F=\frac{\partial F}{\partial x}=0$;

Simply-supported edge: The displacement and moment along the edge are zero, i.e. $F=\frac{\partial^2 F}{\partial x^2}=0$;

Free edge: The moment and shear force along the edge are zero, i.e. $\left(\frac{\partial^2 F}{\partial x^2}+\nu\frac{\partial^2 F}{\partial y^2}\right)_{x=0}=0$ and $\left[\frac{\partial^3 F}{\partial x^3}+(2-\nu)\frac{\partial^3 F}{\partial x\partial y^2}\right]_{x=0}=0$.

2.2. Energy method

Proposed by D.C.L. Rayleigh, the energy method can approximate the minimum natural frequency of a thin plate. The principle of this method can be summed up in one sentence: During the free vibration of a plate, the instantaneous deflection can be expressed as

$$W(x,y,t)=(A\cos\omega t+B\sin\omega t)F(x,y) \tag{3}$$

where ω is the circular frequency; F(x,y) is the shape function.

Targeting the natural vibration frequency, this paper assumes that the thin plate is vibrating freely under no external load. When the plate passes through the equilibrium position, we have *W=0*, $\sin \omega t = 0$ and $\cos \omega t = \pm 1$. In this case, the speed reaches the maximum $\pm \omega F$, the deformation potential energy stands at zero, and the kinetic energy reaches the maximum:

$$T_{\max} = \frac{1}{2} \iint \overline{m} \omega^2 F^2 dxdy \tag{4}$$

When the vibrating plate reaches the farthest distance from the equilibrium position, we have $W = \pm F$, $\sin \omega t = \pm 1$ and $\cos \omega t = 0$. In this case, the kinetic energy of the plate was zero, while the deformation potential energy reaches the maximum:

$$U_{\max} = \frac{D}{2} \iint \left\{ (\nabla^2 W)^2 - 2(1-\nu) \left[\frac{\partial^2 W}{\partial x^2} \frac{\partial^2 W}{\partial y^2} - (\frac{\partial^2 W}{\partial x \partial y})^2 \right] \right\} dxdy \tag{5}$$

According to Green's theorem, we have:

$$\iint \left[\frac{\partial^2 W}{\partial x^2} \frac{\partial^2 W}{\partial y^2} - (\frac{\partial^2 W}{\partial x \partial y})^2 \right] dxdy = \int \left[\frac{\partial W}{\partial x} \frac{\partial^2 W}{\partial x \partial y} dx + \frac{\partial W}{\partial x} \frac{\partial^2 W}{\partial y^2} dy \right] \tag{6}$$

For a rectangular thin plate with no free edge, but simply-supported and fixed edges, $dx = 0$, $\frac{\partial^2 W}{\partial y^2} = 0$, $dy = 0$ and $\frac{\partial W}{\partial x} = 0$ are valid on the boundary with X being constant. Thus, equation (5) can be simplified as:

$$U_{\max} = \frac{D}{2} \iint (\nabla^2 W)^2 dxdy \tag{7}$$

According to the law of conservation of energy, the maximum kinetic energy equals the maximum potential energy:

$$U_{\max} = T_{\max} \tag{8}$$

Then, the natural vibration frequency can be obtained from equation (8).

2.3. Calculation formulas for the natural vibration frequency of rectangular thin plate

The energy method was adopted to compute the minimum natural vibration frequency in engineering (Chang, 2012; Xu *et al.*, 2000). Generally speaking, the shape function (displacement function) of each vibration mode is required to satisfy the displacement boundary condition, but not required to meet the internal force

boundary condition. This is because the latter, an equilibrium condition, is replaced with the energy relationship in the energy method. Of course, the minimum natural vibration frequency is more accurate if the shape function can partially or fully satisfy the internal force boundary condition. The accuracy of the shape curve directly bears on that of the vibration frequency. Under the assumed shape functions, the calculation formulas for the natural vibration frequencies were derived for rectangular thin plates supported on the four sides in six different modes (Figures 1(a)~(f)).

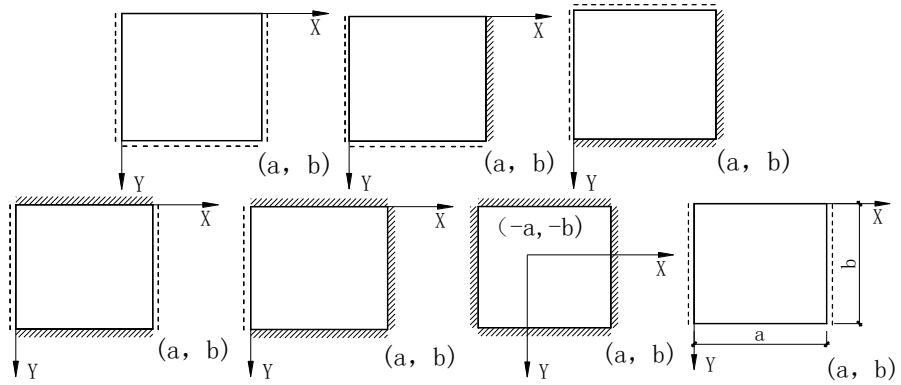

(a) Simply-supported on four sides; (b) Simply-supported on three sides and fixed on one side; (c) Simply-supported on adjacent sides and fixed on the other sides; (d) Simply-supported on one pair of opposite sides and fixed on the other pair; (e) Simply-supported on one side and fixed on three sides; (f) Fixed on four sides; (g) Simply-supported on one pair of opposite sides and free on the other pair

Figure 1. Plates with different supports

2.3.1. Rectangular thin plate simply-supported on four sides

The shape function of the vibration mode for this type of plate was established based on the double trigonometric series proposed by C.L. Navier: $F=\sum_{m=1}^{\infty}\sum_{n=1}^{\infty}C_{mn}\sin\frac{m\pi x}{a}\sin\frac{n\pi x}{b}$ · Under the displacement boundary condition, substituting the shape function into equations (4) and (5), we have:

$$T_{\max}=\frac{\omega^2\overline{m}ab}{8}\sum_{m=1}^{\infty}\sum_{n=1}^{\infty}C_{mn}^2,U_{\max}=\frac{\pi^4abD}{8}\sum_{m=1}^{\infty}\sum_{n=1}^{\infty}C_{mn}^2\left(\frac{m^2}{a^2}+\frac{n^2}{b^2}\right)^2$$

Let m=n=1. Then, the minimum natural frequency can be obtained from equation (8):

$$\omega_1=\pi^2\left(\frac{1}{a^2}+\frac{1}{b^2}\right)\sqrt{\frac{D}{\overline{m}}} \tag{9}$$

Owing to the accuracy of the shape function, which satisfies both displacement boundary condition and internal force boundary condition, the calculated vibration frequency must be accurate.

2.3.2. Simply-supported on three sides and fixed on one side

The shape function $F=\left(2x^4-3ax^3+a^3x\right)\sin\frac{\pi y}{b}$ satisfies the boundary conditions for three-side simple supports ($x=0$, $y=0$, $y=b$) and one-side fixed support ($x=a$). From equations (4), (5) and (8), we have:

$$T_{\max}=\frac{19\omega^2\overline{m}}{4\times630}a^9b, U_{\max}=\frac{Da^5b}{4}\left(\frac{36}{5}+\frac{19\pi^4a^4}{630b^4}+\frac{24\pi^2a^2}{35b^2}\right)$$

$$\omega_1=\frac{1}{a^2}\sqrt{\frac{126}{19}\left(36+\frac{24\pi^2a^2}{7b^2}+\frac{19\pi^4a^4}{126b^4}\right)}\sqrt{\frac{D}{\overline{m}}} \tag{10}$$

2.3.3. Simply-supported on adjacent sides and fixed on the other sides

The mode function $F=C_1(2x^4-3ax^3+a^3x)(2y^4-3by^3+b^3y)$ satisfies the boundary conditions for adjacent-side simple supports ($x=0$, $y=0$) and adjacent-side fixed supports ($x=a$, $y=b$). From equations (4), (5) and (8), we have:

$$T_{\max}=\frac{19\omega^2\overline{m}}{2\times630^2}a^9b^9, U_{\max}=\frac{Da^5b^5}{2}\left(\frac{36\times19}{5\times630}a^4+\frac{36\times19}{5\times630}b^4+\frac{2\times12^2}{35^2}a^2b^2\right)$$

$$\omega_1=\frac{6}{a^2}\sqrt{\frac{126}{19}\left(1+\frac{144a^2}{133b^2}+\frac{a^4}{b^4}\right)}\sqrt{\frac{D}{\overline{m}}} \tag{11}$$

2.3.4. Simply-supported on one pair of opposite sides and fixed on the other pair

The mode function $F=\sin\frac{\pi x}{a}\left(1-\cos\frac{2\pi y}{b}\right)$ satisfies the boundary conditions for opposite-side simple supports ($x=0$, $x=a$) and opposite-side fixed supports ($y=0$, $y=b$). From equations (4), (5) and (8), we have:

$$T_{\max}=\frac{3\omega^2\overline{m}}{2\times4}ab, U_{\max}=\frac{Dab}{2}\left(\frac{3\pi^4}{4a^4}+\frac{4\pi^4}{b^4}+\frac{2\pi^4}{a^2b^2}\right)$$

$$\omega_1=\frac{\pi^2}{a^2}\sqrt{1+\frac{8a^2}{3b^2}+\frac{16a^4}{3b^4}}\sqrt{\frac{D}{\overline{\mathrm{m}}}} \tag{12}$$

2.3.5. Simply-supported on one side and fixed on three sides

The mode function $F=\left(2x^4-3ax^3+a^3x\right)\left(1-\cos\frac{2\pi y}{b}\right)$ satisfies the boundary conditions for one-side simple support ($x=a$, $y=0$, $y=b$) and three-side fixed supports ($x=0$). From equations (4), (5) and (8), we have:

$$T_{\max}=\frac{3\times19\omega^2\overline{m}}{4\times630}a^9b,$$

$$U_{\max}=\frac{Da^5b}{2}\left(\frac{36\times3}{5\times2}+\frac{16\times19\pi^4a^4}{2\times630b^4}+\frac{2\times24\pi^2a^2}{35b^2}\right)$$

$$\omega_1=\frac{1}{a^2}\sqrt{\frac{420}{19}\left(\frac{54}{5}+\frac{48\pi^2a^2}{35b^2}+\frac{152\pi^4a^4}{630b^4}\right)}\sqrt{\frac{D}{\overline{m}}} \tag{13}$$

2.3.6. Fixed on four sides

As shown in Figure 1(f), the side lengths of the rectangular thin plate are 2a and 2b. Then, the mode function $F=C_1\left(x^2-a^2\right)^2\left(y^2-b^2\right)^2$ can satisfy the boundary conditions for four-side fixed supports. From equations (4), (5) and (8), we have:

$$T_{\max}=\frac{2^{15}\omega^2\overline{m}}{81\times25\times49}a^9b^9,$$

$$U_{\max}=\frac{2^{14}Da^5b^5}{9\times25\times7}\left(a^4+b^4+\frac{4}{7}a^2b^2\right)$$

$$\omega_1=\frac{1}{a^2}\sqrt{\frac{63}{2}\left(1+\frac{4a^2}{7b^2}+\frac{a^4}{b^4}\right)}\sqrt{\frac{D}{\overline{m}}} \tag{14}$$

Through the above analysis, the author obtained the calculation formulas for the natural vibration frequencies of rectangular thin plates supported on the four sides in six different modes. However, the boundary conditions for the plate simply-supported on one pair of opposite sides and free on the other pair were not discussed due to the absence of free sides of the rectangular thin plate. To make up for this gap, the natural vibration frequency under the boundary conditions (Figure 1(g)) was derived below.

Equation (2) is the differential equation of the lateral free vibration of plate. The classical expression of the mode function under the boundary conditions is as follows:

$$F=\left(A_m sh\alpha_1 y+B_m ch\alpha_1 y+C_m\sin\alpha_2 y+D_m\cos\alpha_2 y\right)\sin\alpha x \tag{15}$$

where $\alpha=m\pi/a$, $\alpha_1=\sqrt{\gamma^2+\alpha^2}$ and $\alpha_2=\sqrt{\gamma^2-\alpha^2}$. Equation (15) satisfies the vibration differential equation and the boundary conditions $x=0$, $x=a$. According to

the boundary conditions *y=0, y=b*, four homogeneous linear equations with A_m, B_m, C_m *and* D_m as unknown variables, which are not all zero, can be obtained. Thus, the natural frequency equation can be derived as (Xu *et al*., 2000):

$$2\alpha_1\alpha_2\left[\gamma^4-(\mu-1)^2\alpha^4\right]^2\left(ch\alpha_1 b\cos\alpha_2 b-1\right)+$$
$$\left\{\alpha_a^2\left[\gamma^2+(1-\mu)\alpha^2\right]^4-\alpha_1^2\left[\gamma^2+(\mu-\mu 1)\alpha^2\right]^4\right\}sh\alpha_1 b\sin\alpha_2 b=0 \quad (16)$$

For a given value of m, the natural frequencies ω_{m1}, ω_{m2} and ω_{m3} can be calculated by equation (16). The frequencies are fundamental frequencies at m=1. The shape function in equation (15) must satisfy $m<\frac{\gamma a}{\pi}$, that is, $\omega>\frac{m^2\pi^2}{a^2}\sqrt{\frac{D}{m}}$. Thus, it is traditionally held that the minimum natural frequency of the plate equals the natural frequency of a simply-supported beam:

$$\omega_1=\frac{m^2\pi^2}{a^2}\sqrt{\frac{D}{m}} \quad (17)$$

Overall, the author obtained the calculation formulas for the natural vibration frequencies of rectangular thin plates under seven boundary conditions.

3. Experimental introduction

The test site is a certain subway line in Shanghai. There are 2 ordinary masonry structure residential buildings in the test site. In this paper, building NO.2 is used as the research object (Xia and Qu, 2016; Xia *et al*., 2013; Xia and Wu, 2014; Xia, 2014). See in Figure 2. The building with 5-story masonry structure is located at 10m away from the center line of the subway. It was built in the 1960s. The name and plane layout of each room in the building are given in Figure 3. The building has two kinds of floor slabs: precast plates and cast-in-situ plates. Each precast plate is free on a pair of opposite sides and simply-supported on the other, while each cast-in-situ plate is fixed on four sides. In order to compare the vibration of different slab room, tow typical rooms (kitchen room5 (C5), toilet 9 (W9)) are selected in each floor. Among them, C5 are precast slab rooms, and W9 is cast-in-place slab room. The sensors are arranged on the indoor floor panels of each room, and the vertical direction (Z direction) are tested. The average value of more than 10 trains at the same measuring point is analyzed.

The test instrument uses a high-sensitivity piezoelectric accelerometer of French Lance (LC0132T) with a sensitivity coefficient of 49V/g, and an intelligent data acquisition system. Each instrument and sensor were debugged and calibrated before the experiment. In this paper, the test data was filtered and the acceleration signal was recorded.

(a) North facade (b) South facade

Figure 2. Residential building 2#

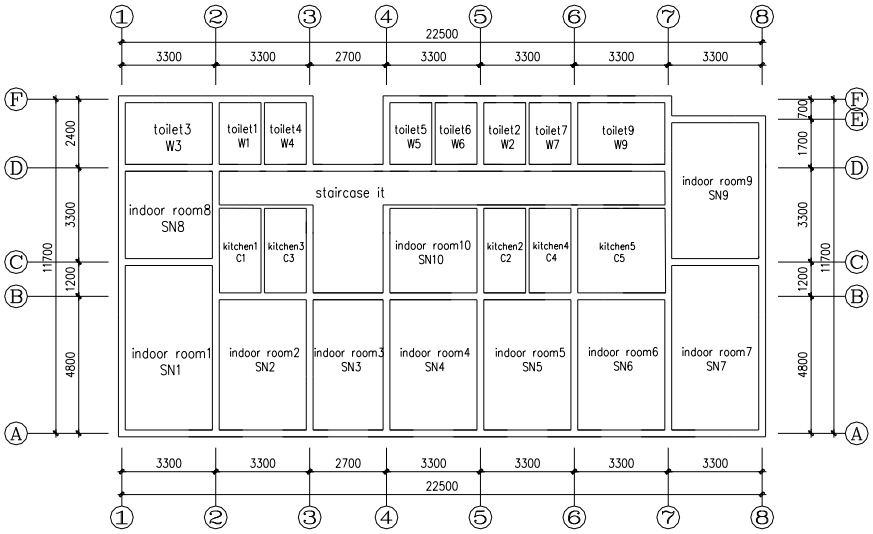

Figure 3. Name and plane layout of each room

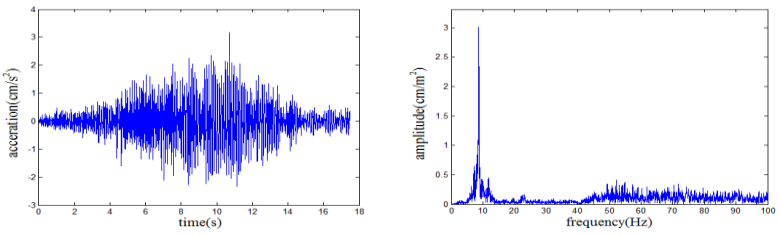

(a) Acceleration time history and frequency spectrum of C5

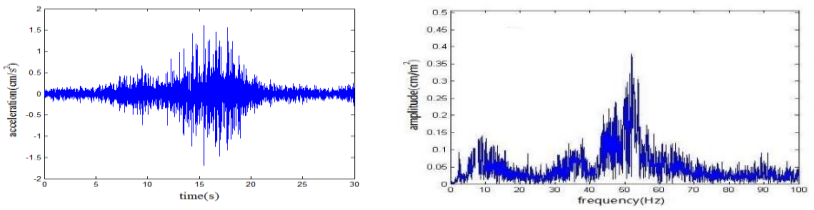

(b) Acceleration time history and frequency spectrum of W9

Figure 4. Mid-span acceleration time history and frequency spectrum on the top floor

Figure 4 shows the acceleration time history and frequency spectrum of room C5 and W9 when the metro passes by. The space limit is limited, only the vibration of the top floor of slab is listed. It can be observed from the picture that the influence of train passing on building vibration is about 10 seconds. In vibration frequency band, the floor slab vibration in kitchen C5 mainly occurred in 5~15Hz, while that in bathroom W9 mainly occurred in 45~55Hz.

4. Natural vibration frequency of rectangular thin plate

Several typical rooms were selected for calculation to obtain the natural vibration frequency of the floor slabs. The plates are made of concrete. The other parameters are as follows: $E = 0.912 \times 10^4 MPa$, $v = 0.2$ and $\rho = 2500 kg/m^3$.

4.1. Precast plate rooms

Three precast plate rooms were selected, including bedroom 1 (SN1), bedroom 2 (SN2) and kitchen 5 (C5). The sizes of these rooms are respectively 3.3m×6m, 3.3m×4.8m and 3.3m×3.15m. Each precast plate is free on a pair of opposite sides and simply-supported on the other. According to equation (17), the natural vibration frequency of the plate is only related to the span. Thus, the three rooms must share the same natural vibration frequency.

Bending stiffness of the plate: $D = \frac{Eh^3}{12(1-v^2)} = \frac{0.912\times10^4\times10^6\times0.1^3}{12(1-0.2^2)} = 791666.67$;

Plate mass per unit area (thickness: 100): $\overline{m} = 164.2 kg/m^2$;

Circular frequency of the plate: $\omega_1 = \frac{\pi^2}{a^2}\sqrt{\frac{D}{m}} = \frac{\pi^2}{3.3^2}\sqrt{\frac{791666.67}{164.2}} = 62.9$;

Natural vibration frequency of the plate: $f = \frac{\omega}{2\pi} = \frac{62.9}{2\pi} = 10.01Hz$.

4.2. Cast-in-situ plate room

One cast-in-situ plate room was selected, namely, bathroom 9 (W9). The size of the room is 2a×2b=3.3m× 2.4m. Each cast-in-situ plate is fixed on all four sides. Thus, the natural vibration frequency was calculated according to equation (14).

Bending stiffness of the plate: $D = \frac{Eh^3}{12(1-v^2)} = \frac{0.912\times10^4\times10^6\times0.1^3}{12(1-0.2^2)} = 791666.67$;

Plate mass per unit area (thickness: 100): $\overline{m} = \rho h = 2500\times0.1 = 250kg/m^2$;

Circular frequency of the plate:

$$\omega_1 = \frac{1}{a^2}\sqrt{\frac{63}{2}\left(1+\frac{4a^2}{7b^2}+\frac{a^4}{b^4}\right)}\sqrt{\frac{D}{\overline{m}}}$$

$$= \frac{1}{(3.3/2)^2}\sqrt{\frac{63}{2}\left(1+\frac{4}{7}\left(\frac{3.3/2}{2.4/2}\right)^2+\left(\frac{3.3/2}{2.4/2}\right)^4\right)}\sqrt{\frac{791666.67}{250}} = 275.85Hz$$

;

Natural vibration frequency of the plate: $f = \frac{\omega}{2\pi} = \frac{275.85}{2\pi} = 43.9Hz$.

5. Numerical model

The finite-element model of precast plate is shown in Figure 5(a). Inspired by Reference (Office of the building standard design co-operation group in the south China area. 03ZG401, 2003), the precast plate (size: 3.3m×0.5m; thickness: 0.1m) of concrete ($E=0.912\times10^4MPa$, v=0.2 and ρ=2500kg/m^3) was simulated as beam units with 5 holes (diameter: 0.08m). The boundaries along the span were treated as simply-supported, while those vertical to the span were treated as free. The first-order natural vibration frequency of 9.85Hz was extracted for modal analysis, which is basically in line with the result of the energy method (10.01Hz).

The finite-element model of cast-in-situ plate is shown in Figure 5(b). The cast-in-situ plate was 3.3m×2.4m in size. The other parameters are the same as those of the precast plate. The plate was simulated as SHELL181 units and the four sides were treated as fixed. The first-order natural vibration frequency of 43.244Hz was extracted for modal analysis, which is basically in line with the result of the energy method (43.9Hz).

Hence, that the natural vibration frequency of precast plate rooms was estimated as 10Hz and that of cast-in-situ plate rooms was estimated as 43Hz for the target residential building.

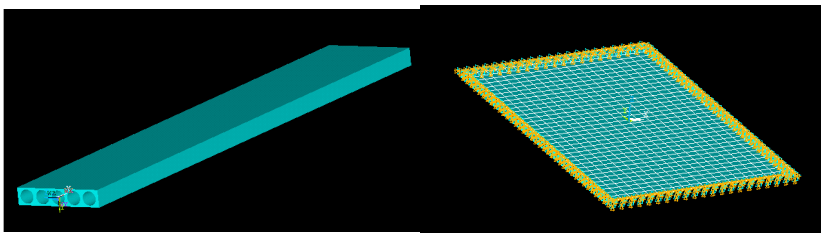

(a)Precast plate model (b) Cast-in-situ plate model

Figure 5. Numerical model of floor slab

6. Floor slab vibration induced by urban traffic

The vibration in buildings is mainly caused by urban traffic, earthquake and nearby construction. For urban traffic-induced vibrations, the surface vibration frequency caused by metro falls in 40~90Hz, in which 60~80Hz corresponds to the highest vibration level, and low-frequency vibrations dominant the vibrations transmitted to buildings (Lou *et al*., 2009; Yan *et al*., 2006); the surface vibration frequency caused by surface vehicles falls in 10~20Hz (Zong *et al*., 2017), that caused by trains falls in 10~100Hz (Xia, 2010), and that caused by elevated road traffic falls in 5~45Hz (Chang *et al*., 2008). For earthquake-induced vibrations, the main frequency is usually below 5Hz. For construction-induced vibrations, the surface vibration frequency caused by blasting falls in 15~45Hz, but the main oscillation (≤0.5s) lasts much shorter than earthquake-induced vibrations (Shen *et al*., 2002), that caused by static piling falls in 4~7Hz (Yao *et al*., 2013), and that caused by hammer and vibration piling falls in 10~30Hz and occurs 2~3m away from the vibration source, indicating that the construction-induced foundation vibration has little impact on nearby buildings (Wang and Tang, 2005). To sum up, the surface vibrations caused by different factors differ greatly in the main frequency band.

The residential building 2# was subjected to field measurement and numerical simulation in References (Xia *et al.*, 2013; Xia and Qu, 2014; Xia, 2014), yielding the Fourier frequency spectra of the typical rooms with precast and cast-in-situ plates in each layer under the excitation of metro and surface vehicles. Due to space limitation, only the simulated results of C5 and W9 on the top floor are presented in Figure 6. Through the analysis, it is concluded that, under the urban traffic excitation, the rooms at the same position of different floors carry great resemblance in vibration frequency band: the floor slab vibration in kitchen C5 mainly occurred in 10~20Hz, while that in bathroom W9 mainly occurred in 45~55Hz.

In Section 4, the natural vibration frequencies of precast plate and cast-in-situ plate rooms are theoretically calculated as 10.01Hz and 43.9Hz. Through analysis, it is learned that the natural vibration frequency of precast plate falls in the range of frequency bands for the floor slab vibrations in precast plate rooms caused by urban traffic, while that of cast-in-situ plate also falls near the corresponding range caused by urban traffic. The results show that urban traffic excitation can induce the

resonance of precast plate, and slightly boost the vibration of cast-in-situ plate (although unable to induce the resonance of the latter plate). Under urban traffic excitation, the vibration amplitude of precast plate is much higher than that of cast-in-situ plate. The result agrees well with the conclusion on plate material properties: “the vertical vibration strength of precast plate room should be greater than that of cast-in-situ plat room in structural design”.

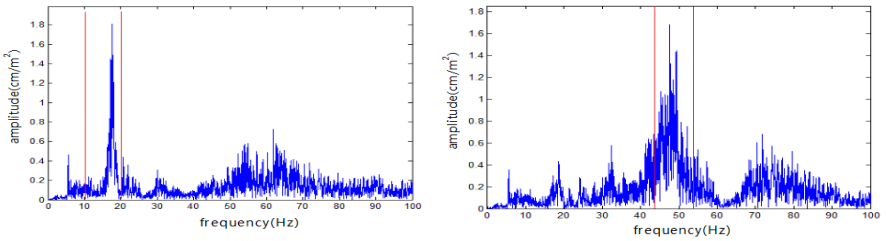

(a) Mid-span Fourier frequency spectrum of precast plate (C5) on the top floor

(b) Mid-span Fourier frequency spectrum of cast-in-situ plate (W9) on the top floor

Figure 6. Fourier frequency spectra of the typical rooms on the top floor

In Section 4, the natural vibration frequencies of precast plate and cast-in-situ plate rooms are theoretically calculated as 10.01Hz and 43.9Hz. Through analysis, it is learned that the natural vibration frequency of precast plate falls in the range of frequency bands for the floor slab vibrations in precast plate rooms caused by urban traffic, while that of cast-in-situ plate also falls near the corresponding range caused by urban traffic. The results show that urban traffic excitation can induce the resonance of precast plate, and slightly boost the vibration of cast-in-situ plate (although unable to induce the resonance of the latter plate). Under urban traffic excitation, the vibration amplitude of precast plate is much higher than that of cast-in-situ plate. The result agrees well with the conclusion on plate material properties: “the vertical vibration strength of precast plate room should be greater than that of cast-in-situ plat room in structural design”.

7. Conclusions

(1) The calculation formulas of natural vibration frequencies of concrete floor slabs were obtained under seven boundary conditions by the energy method, and adopted to determine the natural vibration frequencies of floor slabs in typical rooms of a residential building. It is estimated that the natural vibration frequency of precast plate room is about 10.01Hz and that of cast-in-situ plate room is about 43.9Hz. The estimation is basically in line with the simulated results on floor slabs of the same parameters, indicating that the natural vibration frequencies acquired by the energy method are correct.

(2) The calculated natural vibration frequency of precast plate falls in the frequency range of floor slab vibrations induced by urban traffic. Thus, the precast plate vibration must be caused by urban traffic excitation. To control the vibration, the resonance should be prevented by enhancing or changing the natural vibration frequency of the plate or the overall structure. The calculated natural vibration frequency of cast-in-situ plate falls near the frequency range of floor slab vibrations induced by urban traffic, indicating that urban traffic excitation can slightly boost the vibration of cast-in-situ plate (although unable to induce the resonance of the latter plate).

(3) The proposed calculation method for natural vibration frequency lays the basis for computing the natural vibration frequency of the floor slab in buildings under varied conditions, and judging if the slab vibration is caused by urban traffic excitement. If the vibration is indeed induced by urban traffic, resonance may occur when the natural vibration frequency of the floor slab is close to the frequency of urban traffic-induced vibration transmitted to the building. To weaken the slab vibration induced by traffic excitation, the resonance should be prevented by enhancing or changing the natural vibration frequency of the slab or the overall structure. This conclusion sheds new light on the vibration isolation of the existing structures.

Acknowledgments

This work is supported by the national natural science fund (51708450); China Postdoctoral Science Foundation Project (2018M643702); Basic Research Project of Natural Science in Shaanxi Province(2018JQ5169); Shaanxi Provincial Postdoctoral Foundation Project; Ph. D. Research Start-up Project (107-451115002); School-level Scientific Research Project (2016CX025).

References

Chang L., Ren M., Yan W. M. (2008). In situ experiment and of vibration induced by urban road and elevated road transit. *Journal of Beijing University of Technology*, Vol. 34, No. 10, pp. 1053-1058. http://doi.org/10.1631/jzus.A0720090

Chang W. H. (2012). Calculation of the natural vibration frequency of rectangular thin plates with four edges supported. *Shanxi Architecture*, Vol. 38, No. 5, pp. 63-65.

Hassan O. (2008). Train-Induced ground borne vibration and noise in buildings. *Multi-Science publishing Co.Ltd.UK*.

Lou M. L., Jia X. P., Yu J. Q. (2009). Field measurement and analysis of ground vibration induced by subway trains. *Journal of Disaster Prevention and Mitigation Engineering*, Vol. 29, No. 3, pp. 282-288. http://doi.org/10.1109/CLEOE-EQEC.2009.5194697

Office of the building standard design co-operation group in the south China area. 03ZG401, (2003). *Prestressed concrete hollow slab. Office of Central South area Building Standards Design team.*

Shen L. J., Wang X. G., Yu Y. L., Yang X. L., Zhang Y. C. (2002). Monitoring and analysis of impact vibration cause by tippling of a chimney with height of 100 meters. *Engineering Blasting*, Vol. 8, No. 4, pp. 16-19.

Wang B., Tang H. X. (2005). The analysis of vibration effect caused by pile foundation construction. *Chinese and Overseas Architecture*, No. 2, pp. 100-101.

Xia H. (2010). Traffic induced environmental vibrations and controls. *Beijing: Science Press.*

Xia Q. (2014). Study on subway-induced existing building vibration and isolation method. *Shanghai: Tongji University.*

Xia Q., Qu W. J. (2014). Numerical analysis on metro train-induced vibrations and their influences and affecting factors on existing masonry building. *Journal of Vibration and Shock*, Vol. 33, No. 6, pp. 189-194.

Xia Q., Qu W. J. (2016). Experimental and numerical studies of metro train-induced vibrations on adjacent masonry buildings. *International Journal of Structural Stability and Dynamics*, Vol. 16, No. 10, pp. 1550067. http://dx.doi.org/10.1142/S0219455415500674

Xia Q., Qu W. J., Shang X. D. (2013). Test for effects of metro train-induced vibration on existing masonry buildings. *Journal of Vibration and Shock*, Vol. 32, No. 12, pp. 11-16.

Xu Q. L., Zhang F., Ji H. E. (2000). Discussion about the solution of the free vibration frequency of rectangular plate with two opposite ends simply supported and two opposite ends free. *Journal of Zhengzhou University of Technology*, Vol. 21, No. 4, pp. 1-3.

Yan W. M., Zhang Y., Ren M. (2006). In situ experiment and analysis of environmental vibration induced by urban subway transit. *Journal of Beijing University of Technology*, Vol. 32, No. 2, pp. 149-154.

Yao D. P., Zhang Y. F., Ye Y. Q. (2013). Impact of jacked pile construction vibration on environment and its control measures. *Chinese Journal of Underground Space and Engineering*, Vol. 9, No. s1, pp. 1739-1743.

Zong G., Zhang Y. H., Li G. Z. (2017). Measurement and research on metro vibration attenuation law predicted by road traffic. *Chinese Journal of Underground Space and Engineering*, Vol. 13, No. 1, pp. 229-235.